Distributed feedback regime of photonic crystal waveguide lasers at 1.5 μm

X. Checoury,[a] P. Boucaud, and J-M. Lourtioz
Institut d'Électronique Fondamentale, UMR 8622 du CNRS, Bât. 220, Université Paris-Sud, 91405, Orsay Cedex, France

F. Pommereau, C. Cuisin, E. Derouin, O. Drisse, L. Legouezigou, F. Lelarge, F. Poingt, and G. H. Duan
Opto+, Alcatel Research & Innovation, Route de Nozay, 91460, Marcoussis Cedex, France

D. Mulin, S. Bonnefont, O. Gauthier-Lafaye, J. Valentin, and F. Lozes
LAAS-CNRS, 7 Av. du Colonel Roche, 31077 Toulouse Cedex 4, France

A. Talneau
Laboratoire de Photonique et Nanostructures, UPR 20 du CNRS, 91460 Marcoussis Cedex, France

Lasing of W3 and W2/3 triangular lattice photonic crystal waveguides on InP substrate is investigated around 1.5 μm by optical pumping. The lattice period of the fabricated structures is varied from 320 to 540 nm by steps of 20 nm, thereby leading to a detailed exploration of the lasing mechanism over a large frequency range. A distributed-feedback-laser- (DFB-) like-emission is observed above the gap (W3), while a genuine DFB laser emission is obtained in the gap (W2/3). Side-mode suppression ratios can reach 40 dB when an antireflecting coating is used on the cleaved output facet. Experimental results including light–light characteristics are analyzed in the framework of two-dimensional plane-wave calculations. © *2004 American Institute of Physics.* [DOI: 10.1063/1.1832731]

Photonic crystals (PhC) are artificial dielectric structures of great interest for miniature optical devices in integrated optics. Recently, they have been used to fabricate small size, single-mode edge emitting photonic crystal lasers.[1,2] In the first work,[1] the laser design was based on PhC waveguides made of a small number of coupled PhC micro-resonators.[3] The photonic crystal itself was obtained using the substrate approach where holes are etched into a buried planar waveguide with a fairly low vertical confinement. In the second work,[2] the authors used the membrane approach, which is known to provide a much higher vertical confinement, but with the disadvantages of stronger heating effects and of a more difficult implementation in the case where an electrical excitation is used. The lasers relied on ultranarrow PhC waveguides consisting of one row of missing holes (W1) in a perforated membrane.

In this letter, we report an experimental study of medium-size W3 and W2/3 PhC waveguide lasers on InP substrate. The substrate approach is used as in previous works[1,4] for the fabrication of triangular-lattice PhC lasers. The lattice period of all the fabricated structures is varied over a very wide range of values while the amplification band of the active medium is fixed. This allows us a detailed exploration of the laser spectral behavior either within or above the gap. It is shown that W3 lasers can operate above the gap in a distributed-feedback- (DFB-) like-regime with a relatively large side-mode suppression ratio at 1.5 μm. One interest of such a laterally modulated waveguide structure as compared to classical DFB structures stems from the fact that no regrowth is needed during the device fabrication.[5–7] A more particular interest of *two-dimensional* triangular PhC waveguide structures is to operate in a full TE gap with theoretically zero in-plane waveguide losses. It is shown that the fundamental mode folding of W2/3 lasers studied in this work occurs in the gap leading to a genuine DFB emission.

More precisely, the PhC waveguide lasers were fabricated in an InP/InGaAsP/InP laser structure including six compressively strained InGaAsP quantum wells whose emission was centered at 1550 nm. The triangular lattice of holes was defined by electron beam lithography. Different lattice periods were used ranging from 320 to 540 nm by steps of 20 nm. The holes were etched around 4 μm deep through the whole semiconductor heterostructure.[8] The air filling factor was kept to the value of 30%, thus leading to a TE gap only. Waveguides were fabricated in the main crystal directions (ΓK and ΓM) for each PC. As usual, W3 waveguides consist of three rows of missing holes in the ΓK direction. The W2/3 waveguides, oriented in the ΓM direction, present a periodically varying width, alternately determined by two and three missing holes. In our experiments, all the waveguides were ~800 PhC periods long, resulting in an overall laser length in the range from 250 up to 430 μm. The waveguide lasers were terminated with a cleaved facet at one end, and a PhC mirror at the other end. The PhC mirror had the same lattice constant, filling factor, and orientation as the rest of the PhC matrix. Finally, two series of lasers were prepared: (i) with and (ii) without antireflecting (AR) coating on the cleaved facet. A 1.06 μm pulsed YAG laser was used for optical pumping. The pump pulses were 15 ns long, and the pulse repetition rate was 10 kHz. The pump beam was focused with a cylindrical lens onto a ~10-μm-wide, ~2-mm-long light spot. The laser emission was spectrally resolved at the waveguide output using a monochromator.

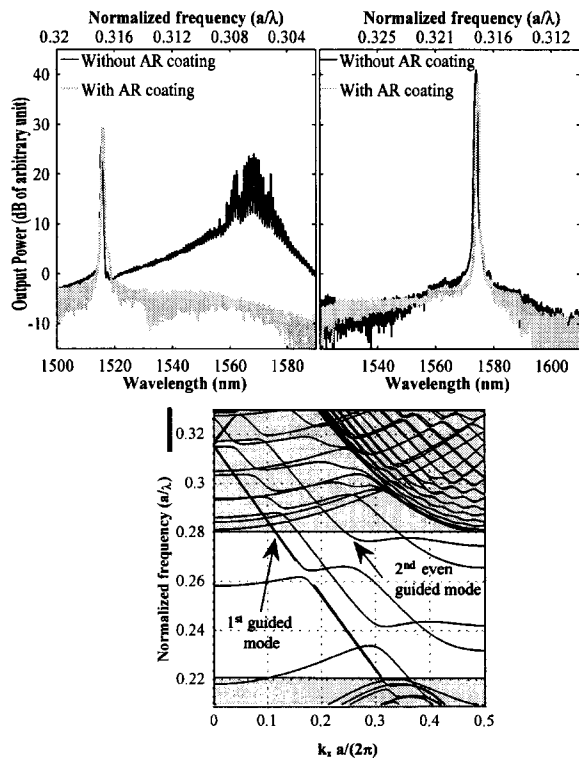[a]Electronic mail: xavier.checoury@ief.u-psud.fr

5502

FIG. 1. Top panel: measured spectra of W3 lasers with and without AR coating (gray and black curves, respectively). Top left: lattice period of 480 nm. Top right: lattice period of 500 nm. Bottom panel: W3 waveguide band diagram (ΓK direction) with the gain region indicated on the left for a PhC period of 500 nm.

Figure 1 (top panel) shows the emission spectra measured at room temperature for two W3 waveguide lasers with lattice constants $a=480$ nm (left) and $a=500$ nm (right), respectively. In both cases, the PhC lasers are pumped near twice above threshold. For $a=480$ nm, the spectrum in the absence of AR coating consists of a solitary peak at $\lambda=1515$ nm (i.e., $a/\lambda=0.317$) along with multiple peaks ranging from 1550 to 1580 nm (i.e., $0.30 \leqslant a/\lambda \leqslant 0.31$). A DFB-like mode is actually in competition with Fabry–Perot (FP) modes. As seen, the FP modes are regularly spaced from each other, and the wavelength separation (~ 0.85 nm) corresponds to an effective group index of 3.67 for a cavity length of 392 μm. These modes vanish in the presence of AR coating while the DFB mode still lases. A similar behavior of FP modes has been obtained for any PhC period smaller than 480 nm. For $a=500$ nm (Fig. 1, top right), the laser spectrum is single mode whether an AR coating is used or not. The DFB-like mode now occurs at gain maximum ($\lambda=1575$ nm, i.e., $a/\lambda=0.317$). The side-mode suppression ratio is as large as 40 dB.

In order to explain the laser spectra of Fig. 1, the band diagram of the W3 waveguide was computed using a two-dimensional plane wave expansion with the supercell method.[9] The effective index was calculated to be 3.21. The air filling factor was 30% as in the experiments. The results of calculations are shown in Fig. 1 (bottom panel). The dispersion curve of the lowest order guided mode is represented in thick lines. The white area delimits the TE gap of the triangular lattice that extends from $a/\lambda=0.22$ to $a/\lambda=0.28$. As seen, the normalized frequency calculated for the second folding of the fundamental mode dispersion curve ($a/\lambda=0.315, k=0$) is in good agreement with the one measured
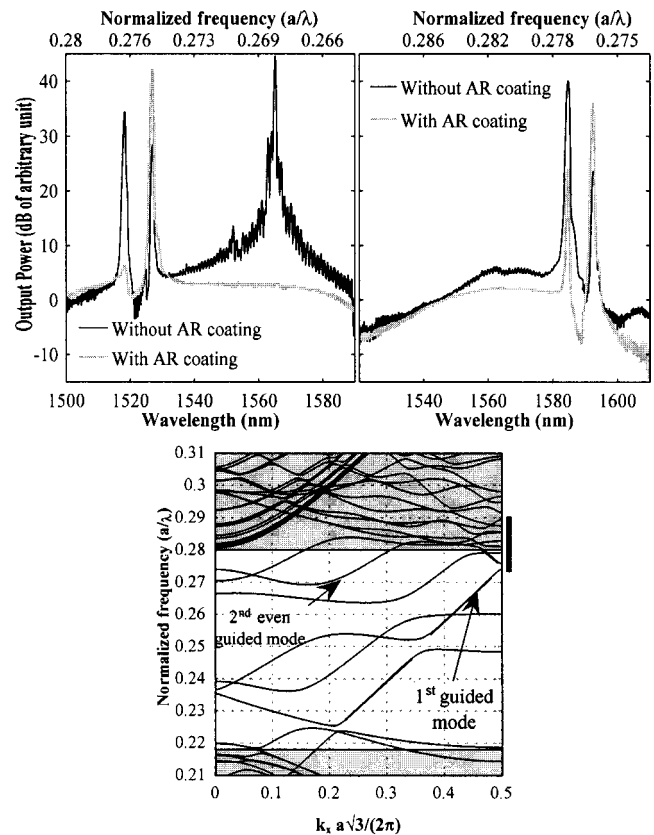

FIG. 2. Top panel: measured spectra of W2/3 lasers with and without AR coating (gray and black curves, respectively). Top left: lattice period of 420 nm. Top right: lattice period of 440 nm. Bottom panel: W2/3 waveguide band diagram (ΓM direction) with the gain region indicated on the right for a PhC period of 440 nm.

for the DFB line (Fig. 1, top). Indeed, the W3 laser behaves as a second-order DFB laser. The band diagram also reveals the opening of a narrow stop-band whose calculated width is $\Delta\lambda=1.7$ nm. Actually, calculations of the two-dimensional (2D) mode patterns show that only the low frequency DFB mode is well confined in the guide. In contrast, the high frequency mode spreads in the PhC walls of the guide, and likely suffers large diffraction losses. This explains why the laser seems to be intrinsically single mode.

Figure 2 (top panel) shows the emission spectra measured at room temperature for two W2/3 PhC waveguide lasers with lattice constants $a=420$ nm (left) and $a=440$ nm (right), respectively. Both PhC lasers are pumped near twice above threshold, the value of which is similar to that of W3 lasers. Unlike the spectra of Fig. 1 (top left), those of Fig. 2 (top left) reveal the presence of two modes that coexist with FP modes. The FP mode spacing (~ 1 nm) approximately corresponds to an effective group index of 3.80 for a cavity length of 320 μm. The two main modes are actually the two components of a DFB laser emission. Both of them remain active in the presence of AR coating while the FP modes vanish. Such a behavior is observed for any PhC period smaller than 420 nm. For $a=440$ nm (Fig. 2, top right), the two DFB components are dominant whether an AR coating is used or not.

The calculated band diagram of the W2/3 waveguide is reported in Fig. 2 (bottom panel). As seen, the measured DFB emission now corresponds to the third folding of the fundamental mode dispersion curve $[a/\lambda=0.275, k$
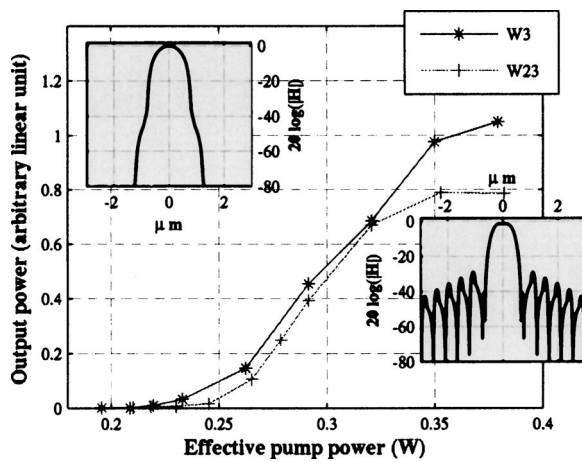
FIG. 3. Light–light characteristics of W3 and W2/3 lasers with PhC periods of 500 and 440 nm, respectively. Top inset: *H*-field profile of the fundamental W3 waveguide mode calculated for $a/\lambda=0.316$ (wave vector $k=0$). Bottom inset: *H*-field profile of the fundamental W2/3 waveguide mode calculated for $a/\lambda=0.276$ [wave vector $k=\pi/(a\sqrt{3})$].

$=\pi/(a\sqrt{3})$]. Unlike the W3 case, this folding occurs inside the photonic gap. The calculated frequencies of the two DFB components are in agreement with those measured experimentally (0.277 and 0.275). The W2/3 laser thus behaves as a third-order DFB laser. Here the calculated (and measured) stop-band is much larger than in the W3 case ($\Delta\lambda\approx 8$ nm). Following the coupled mode theory,[10] the coupling coefficient can be evaluated from $\kappa=(\pi n_g\Delta\omega)/a$, where n_g is the effective group index and $\Delta\omega$ the stop-band width in normalized frequency units. The κ coefficient is evaluated to be 400 cm^{-1} from the numerical calculations, which value is quite large. This reflects the strong interaction between the mode field and the photonic crystal as will be shown from the calculated mode profile (Fig. 3, right inset).

Band diagrams also help us to identify the FP lasing mode(s) in the absence of AR coating. In the W3 case and for $a=480$ nm (Fig. 1, top left), three guided modes can contribute to the FP-type emission, i.e., the first two even modes and the first odd mode. The effective group indexes of these modes are, respectively, calculated to be 3.28, 3.88, and 3.5 from the numerical model,[9] while the experimental group index deduced from the FP fringe separation in Fig. 1 (top left) is ≈ 3.67. Therefore, all three modes can be considered. However, the relative regularity of the FP spectrum indicates that one mode is dominant. As is most probable, this mode is the first even one. In the W2/3 case and for $a=420$ nm (Fig. 2, top left), two modes can contribute to the low-frequency part of the FP-type spectrum ($0.264 \leqslant a/\lambda < 0.268$), i.e., the first even mode and the first odd mode. The effective group indexes of these modes are, respectively, calculated to be 3.45 and 5.1 from Fig. 2 (bottom), while the experimental group index deduced from the FP fringe separation in Fig. 2 (top left) is ≈ 3.85. Only the first even mode is thus lasing. The relatively small discrepancy between the theoretical and experimental group index values is readily explained by the measurement uncertainty as well as the overall simplifications of the 2D model. In the high frequency region ($a/\lambda > 0.268$), the second even mode is also allowed as shown in Fig. 2 (bottom). Moreover, its group velocity is very low, which enhances its interaction

with the gain medium.[11] This likely explains the stronger spikes observed in the FP-type spectrum at certain frequencies ($a/\lambda\approx 0.268$ or 0.270).

Figure 3 shows the powers measured on the DFB lasing modes (Figs. 1 and 2, top right) versus the effective power deposited in the active layers over a $\sim 10\times 400~\mu m^2$ surface. Because the pump laser is pulsed, the DFB laser linewidth is somewhat broadened (to ≈ 0.4 nm) due to transients. The output power is obtained by numerically integrating the measured spectra over ~ 30 nm around the main emission peak(s). As seen in Fig. 3, the W3 and W2/3 lasers exhibit similar thresholds and similar slopes above thresholds, though lasing occurs above and inside the gap, respectively. However, one must notice that the W2/3 waveguide has a narrower width and its fundamental mode is less confined than in the W3 case. This is illustrated in the inset of Fig. 3, which show the transverse mode profile calculated for each case. Larger out-of-plane diffraction losses are thus expected for the W2/3 laser. Moreover, the W2/3 DFB laser emission is more detuned from the gain center than the W3 one. We propose that the in-gap situation compensates for these disadvantages.

In conclusion, lasing of W3 and W2/3 triangular lattice photonic crystal waveguides has been investigated around 1550 nm under optical pumping. A simple PhC lattice was used. We have shown that W3 and W2/3 PhC waveguides can behave either as Fabry–Perot or DFB lasers depending on the PhC period and the use of an AR coating. These experimental results have been well explained from band diagram calculations. For the W3 waveguide oriented in the ΓK direction, contradirectional coupling of the fundamental mode has been shown to occur above the gap with low propagation losses, but with a relatively poor feedback. For the W2/3 waveguide oriented in the ΓM direction, a stronger feedback has been obtained within the gap, but with higher out-of-plane losses. The respective advantages of these two configurations should be possibly combined in future medium-size PhC waveguide lasers using a more sophisticated PhC waveguide pattern.

[1] T. D. Happ, M. Kamp, A. Forchel, J. L. Gentner and L. Goldstein, Appl. Phys. Lett. **82**, 4 (2003).
[2] A. Sugitatsu and S. Noda, Electron. Lett. **39**, 213 (2003).
[3] A. Yariv, Y. Xu, R. K. Lee, and A. Scherer, Opt. Lett. **24**, 711 (1999).
[4] S. Mahnkopf, M. Arlt, M. Kamp, V. Colson, G.-H. Duan, and A. Forchel, IEEE Photonics Technol. Lett. **16**, 353 (2004).
[5] L. M. Miller, J. T. Verdeyen, J. J. Coleman, R. P. Bryan, J. J. Alwan, K. J. Beermink, J. S. Hughes, and T. M. Cockerill, IEEE Photonics Technol. Lett. **3**, 6 (1991).
[6] H. Abe, S. G. Ayling, J. H. Marsh, R. M. De la Rue, and J. S. Roberts, IEEE Photonics Technol. Lett. **7**, 452 (1995).
[7] M. Müller, F. Klopf, M. Kamp, J. P. Reithmaier, and A. Forchel, IEEE Photonics Technol. Lett. **14**, 1246 (2002).
[8] F. Pommereau, L. Legouézigou, S. Hubert, S. Sainson, J-P. Chandouineau, S. Fabre, G-H. Duan, B. Lombardet, R. Ferrini, and R. Houdré, J. Appl. Phys. **95**, 2242 (2004).
[9] S. G. Johnson and J. J. Joannopoulos, Opt. Express **8**, 173 (2001).
[10] S. Olivier, H. Benisty, C. Weisbuch, C. J. M. Smith, T. F. Krauss, and R. Houdre, Opt. Express **11**, 1490 (2003).
[11] K. Sakoda, *Optical Properties of Photonic Crystals* (Springer, Berlin, 2001).